Supporting Information

Designing Two-Dimensional Properties in Three-Dimensional Halide Perovskites via Orbital Engineering

Gang Tang,[†] Zewen Xiao,[‡] and Jiawang Hong*[,†]

[†]School of Aerospace Engineering, Beijing Institute of Technology, Beijing, 100081, China

[‡]Wuhan National Laboratory for Optoelectronics, Huazhong University of Science and Technology, Wuhan 430074, China

*E-mail: hongjw@bit.edu.cn

Computational details

Density-functional theory (DFT) calculations were performed using the projector-augmented wave (PAW) method as implemented in the Vienna Ab initio Simulation Package (VASP) 5.4 code.[1-2] The generalized gradient approximation (GGA) Perdew-Burke-Ernzerhof (PBE) functional[3] was chosen for structural relaxations and total energy calculations. The plane-wave cut-off energy was set to 500 eV. The Γ-centered *k*-point meshes with *k*-spacing of ~0.2 $Å^{-1}$ were employed for sampling the Brillouin zone.[4] The lattice parameters and atomic positions were fully relaxed until the force on each atom is smaller than 0.01 eV/Å. The staring structure of $Cs_2Au(I)Au(III)I_6$ is from Ref. 5. The optimized structural parameters were summarized in Table S4. In order to obtain an accurate description of the electronic structure for $Cs_2Au(I)Au(III)I_6$, the Heyd-Scuseria-Ernzerhof (HSE) hybrid functional[6] was therefore used during band structure and density of states calculations. Based on the equation $m^* = \hbar^2/(\partial^2\varepsilon(k)/\partial k^2)$, where $\varepsilon(k)$ are the band edge eigenvalues and k is the wavevector, the electron and hole effective masses were calculated using the finite difference method.[7] The optical absorption spectra are described by the complex dielectric function, *i.e.*, $\varepsilon(\omega) = \varepsilon_1(\omega) + \varepsilon_2(\omega)$. Based on the obtained dielectric function of $Cs_2Au(I)Au(III)I_6$, the absorption coefficient $\alpha(\omega)$ can be given by the following equation[8]:

$$\alpha(\omega) = \frac{\sqrt{2}\omega\sqrt{\sqrt{\varepsilon_1(\omega)^2 + \varepsilon_2(\omega)^2} - \varepsilon_1(\omega)}}{c} \tag{S1}$$

where ε_1 and ε_2 are the real and imaginary part of the dielectric function, respectively.

Carrier mobilities

The intrinsic carrier mobility of $Cs_2Au(I)Au(III)I_6$ is calculated using the deformation potential (DP) theory[9] according to the following equation[10]:

$$\mu = \frac{(8\pi)^{1/2}\hbar^4 e C_{ii}}{3(m^*)^{5/2}(k_B T)^{3/2}E_1^2} \tag{S2}$$

where $\hbar$ is the reduced Planck constant, e is the element charge, C_{ii} is the elastic matrix constant, m^* is the carrier effective mass, k_B is the Boltzmann constant, T is the temperature. E_1 represents the deformation potential constant of the valence band minimum (VBM) for hole or conduction band maximum (CBM) for electron along the transport direction, defined by $E_1 = \Delta E/(\Delta l/l_0)$. Here ΔE is the energy shift of the CBM or VBM under proper lattice compression or dilatation, l_0 is the lattice constant

in the transport direction and Δl is the deformation of l_0. The temperature used for the mobility calculations was 300 K. Note that, the carrier mobilities along the different transport directions are calculated based on the unit cell of $Cs_2Au(I)Au(III)I_6$.

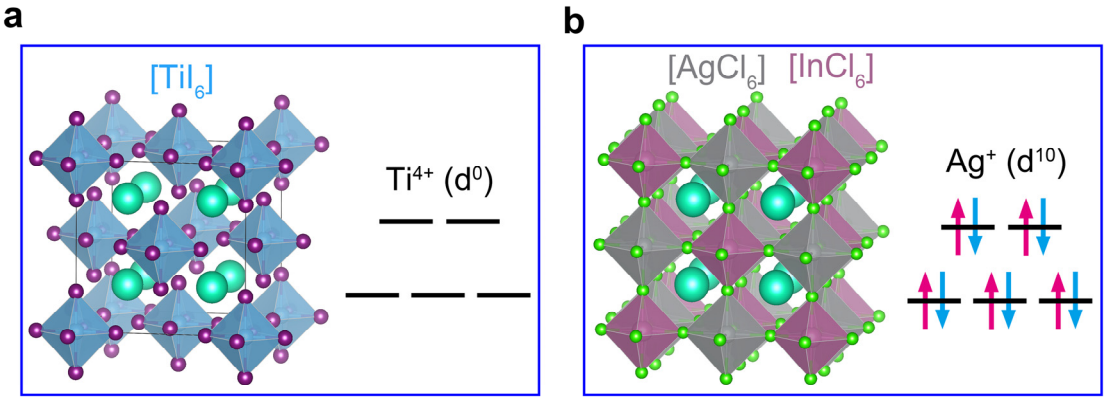

Figure S1. Crystal structures and *d* electron configurations of (a) Cs_2TiI_6 and (b) $Cs_2AgInCl_6$.

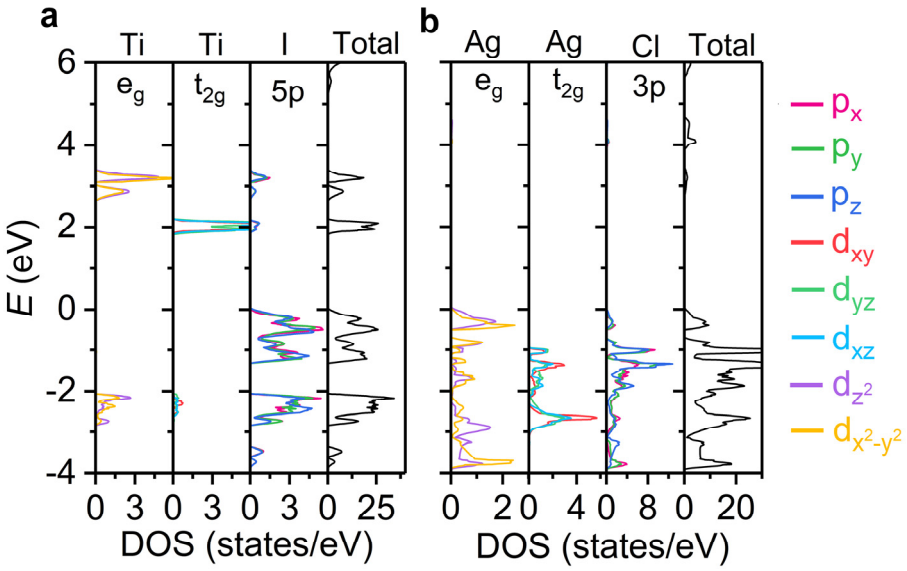

Figure S2. Projected density of states of (a) Cs_2TiI_6 and (b) $Cs_2AgInCl_6$.

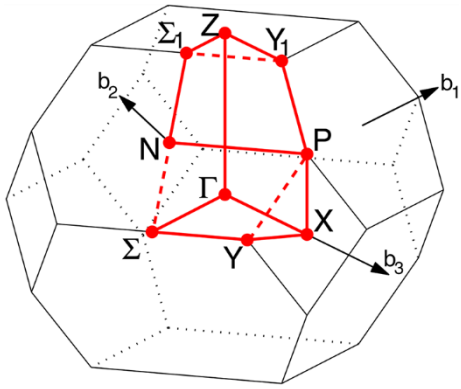

Figure S3. First Brillouin zone for the tetragonal lattice of $Cs_2Au(I)Au(III)I_6$.[11]

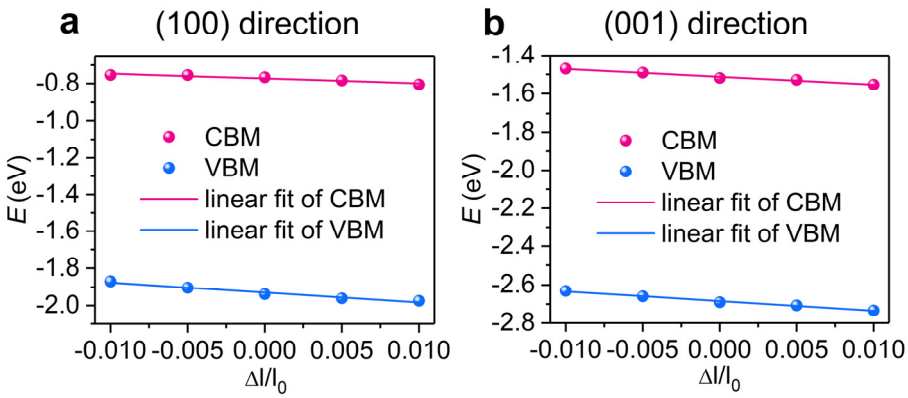

Figure S4. The band-edge positions of VBM and CBM as a function of the lattice dilation along the (100) and (001) directions for $Cs_2Au(I)Au(III)I_6$.

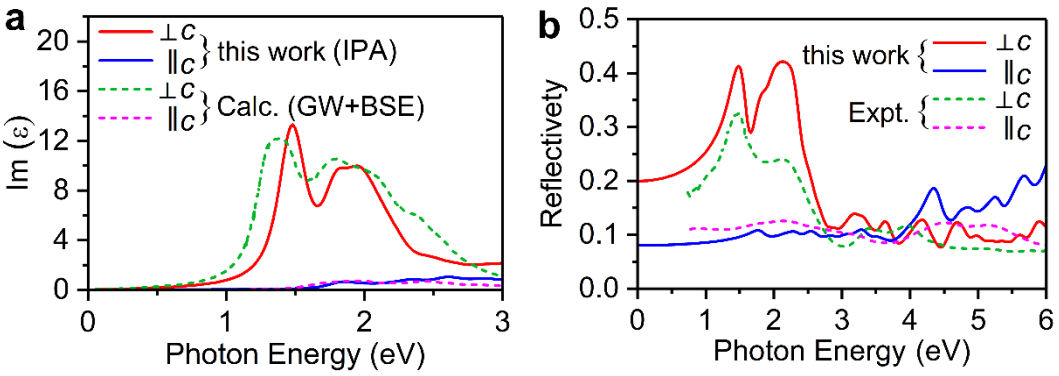

Figure S5. Imaginary part of the macroscopic dielectric function (a) and reflectivity spectra (b) for light polarized parallel and perpendicular to the *c* axis in $Cs_2Au(I)Au(III)_6$. The dashed lines represent the results of the literatures (Ref. 12 in (a) and Ref. 13 in (b)).

Table S1. The ionic (ε_{ion}) and electronic (ε_{∞}) contributions to the static dielectric constant (ε_{std}) for $Cs_2Au(I)Au(III)I_6$.

ε_{ion}^{xx}	ε_{ion}^{yy}	ε_{ion}^{zz}	$\varepsilon_{\infty}^{xx}$	$\varepsilon_{\infty}^{yy}$	$\varepsilon_{\infty}^{zz}$	ε_{std}^{xx}	ε_{std}^{yy}	ε_{std}^{zz}
12.40	12.40	8.71	11.86	11.86	4.23	24.26	24.26	12.94

Table S2. Summary of the calculated and experimental values of elastic constants C_{ij} (GPa) of thirteen halide perovskites.

		C_{11}	C_{33}	C_{44}	C_{66}	C_{12}	C_{13}	C_{14}	Ref.
Calc.	$Cs_2Au_2I_6$ (PBE)	15.53	17.43	0.89	5.84	9.97	1.70	-	This work
	$Cs_2Au_2I_6$ (LDA)	27.67	27.28	2.33	8.12	18.13	3.58	-	This work
	$Cs_2Au_2I_6$ (PBEsol)	29.31	29.07	2.96	9.69	19.37	3.58	-	This work
	Cs_2AgBiI_6	43.68	-	7.48	-	9.04	-	-	14
	$Cs_2AgBiBr_6$	59.02	-	8.15	-	13.37	-	-	14
	$Cs_2TlBiBr_6$	32.71	-	3.16	-	4.41	-	-	15
	$Cs_2AgBiCl_6$	66.70	-	8.85	-	15.61	-	-	14
	$(MA)_2KGdCl_6$	29.33	38.23	13.17	10.76	7.80	18.43	-3.05	16
	$(MA)_2KYCl_6$	30.58	35.32	13.82	10.63	9.32	16.29	-2.61	16
	$(MA)_2KBiCl_6$	31.75	24.79	12.11	10.00	11.75	14.38	-3.58	16
Expt.	$MAPbI_3$	21.8±1.3	-	7.3±0.3	-	11.3±3.1	-	-	17
	$FAPbI_3$	11.1±2.0	-	2.7±0.3	-	-5.5±2.2	-	-	17
	$MAPbBr_3$	34.5±1.2	-	4.1±0.2	-	18.5±2.0	-	-	17
	$FAPbBr_3$	27.7±1.6	-	3.1±0.1	-	11.5±2.4	-	-	17
	$MAPbCl_3$	-	-	3.0(2)	-	-	-	-	18

Table S3. Summary of the calculated and experimental values of bulk modulus *B* (GPa), shear modulus *G* (GPa), Young's modulus *E* (GPa), Pugh's ratio *B*/*G* of twelve halide perovskites.

		Phase	Orientation	B_{VRH} (GPa)	G_{VRH} (GPa)	*E* (GPa)	*B*/*G*	Ref.
Calc.	$Cs_2Au_2I_6$ (PBE)	Tetragonal	-	8.27	2.80	7.54	2.95	This work
	$Cs_2Au_2I_6$ (LDA)	Tetragonal	-	14.51	5.16	13.85	2.81	This work
	$Cs_2Au_2I_6$ (PBEsol)	Tetragonal	-	15.33	5.99	15.89	2.56	This work
	Cs_2AgBiI_6	Cubic	-	16.595	7.5222	19.604	2.20	19
	$Cs_2AgBiBr_6$	Cubic	-	20.269	8.5383	22.461	2.41	19
	$Cs_2AgBiCl_6$	Cubic	-	22.562	9.7791	25.634	2.30	19
	$Cs_2TlBiBr_6$	Cubic	-	13.84	6.07	15.89	2.28	15
	$(MA)_2KGdCl_6$	Trigonal	-	19.63	10.18	26.03	1.93	16
	$(MA)_2KYCl_6$	Trigonal	-	19.7	10.79	27.38	1.83	16
Expt.	$Cs_2AgBiBr_6$	Cubic	(111)		-	22.6(6)	-	14
	$(MA)_2AgBiBr_6$	Cubic	(111)	-	-	7.9	-	20
			(110)	-	-	8.4	-	
	$(MA)_2TlBiBr_6$	Cubic	(111)	-	-	12.8±1.9	-	21
	$(MA)_2KBiCl_6$	Trigonal	(001)	-	-	10.5±1.18	-	16
	$MAPbI_3$	Tetragonal	(100)	-	-	10.4(8)	-	22
			(112)	-	-	10.7(5)	-	
	$FAPbI_3$	Cubic	(100)	-	-	11.8(1.9)	-	23
			(110)	-	-	11.3±0.7	-	
			(012)	-	-	10.2±0.5	-	

Table S4. Experimental and calculated structural parameters for tetragonal phase $Cs_2Au(I)Au(III)I_6$ (space group *I*4/*mmm*). For comparison, the results of the literatures are also given.

	This work (PBE)	This work (LDA)	This work (PBEsol)	Expt. (Ref. 5)	Calc. (Ref. 24)	Calc. (Ref. 12)
a (Å)	8.469	8.145	8.141	8.284	8.39	8.47
b (Å)	8.469	8.145	8.141	8.284	8.39	8.47
c (Å)	12.521	11.937	11.928	12.092	12.34	-
α (deg)	90	90	90	90	90	90
β (deg)	90	90	90	90	90	90
γ (deg)	90	90	90	90	90	90
V ($Å^3$)	898.09	791.98	790.57	829.8	869.04	-
Au(I)-I bond length (Å)	2.618	2.608	2.612	2.586	2.625	2.62
Au(III)-I bond length (Å)	2.700	2.676	2.680	2.646	2.703	2.71

References:

(1) Kresse, G.; Furthmüller, J., Efficiency of Ab-Initio Total Energy Calculations for Metals and Semiconductors Using a Plane-Wave Basis Set. *Comput. Mater. Sci.* **1996**, *6*, 15-50.

(2) Kresse, G.; Joubert, D., From Ultrasoft Pseudopotentials to the Projector Augmented-Wave Method. *Phys. Rev. B* **1999**, *59*, 1758.

(3) Perdew, J. P.; Burke, K.; Ernzerhof, M., Generalized Gradient Approximation Made Simple. *Phys. Rev. Lett.* **1996**, *77*, 3865.

(4) Blöchl, P. E.; Jepsen, O.; Andersen, O. K., Improved Tetrahedron Method for Brillouin-Zone Integrations. *Phys. Rev. B* **1994**, *49*, 16223.

(5) Matsushita, N.; Kitagawa, H.; Kojima, N., A Three-Dimensional Iodo-Bridged Mixed-Valence Gold (I, III) Compound, $Cs_2Au^IAu^{III}I_6$. *Acta Crystallogr., Sect. C: Cryst. Struct. Commun.* **1997**, *53*, 663-666.

(6) Heyd, J.; Scuseria, G. E.; Ernzerhof, M., Hybrid Functionals Based on a Screened Coulomb Potential. *J. Chem. Phys.* **2003**, *118*, 8207-8215.

(7) Whalley, L. D.; Frost, J. M.; Morgan, B. J.; Walsh, A. Impact of Nonparabolic Electronic Band Structure on the Optical and Transport Properties of Photovoltaic Materials. *Phys. Rev. B* **2019**, *99*, 085207.

(8) Jong, U.-G.; Yu, C.-J.; Ri, J.-S.; Kim, N.-H.; Ri, G.-C., Influence of Halide Composition on the Structural, Electronic, and Optical Properties of Mixed $CH_3NH_3Pb(I_{1-x}Br_x)_3$ Perovskites Calculated Using the Virtual Crystal Approximation Method. *Phys. Rev. B* **2016**, *94*, 125139.

(9) Bardeen, J.; Shockley, W., Deformation Potentials and Mobilities in Non-Polar Crystals. *Phys. Rev.* **1950**, *80*, 72.

(10) Wang, L.-Z.; Zhao, Y.-Q.; Liu, B.; Wu, L.-J.; Cai, M.-Q., First-Principles Study of Photovoltaics and Carrier Mobility for Non-Toxic Halide Perovskite $CH_3NH_3SnCl_3$: Theoretical Prediction. *Phys. Chem. Chem. Phys.* **2016**, *18*, 22188-22195.

(11) Setyawan, W.; Curtarolo, S., High-Throughput Electronic Band Structure Calculations: Challenges and Tools. *Comput. Mater. Sci.* **2010**, *49*, 299-312.

(12) Giorgi, G.; Yamashita, K.; Palummo, M., Two-Dimensional Optical Excitations in the Mixed-Valence $Cs_2Au_2I_6$ Fully Inorganic Double Perovskite. *J. Mater. Chem. C* **2018**, *6*, 10197-10201.

(13) Liu, X.; Matsuda, K.; Moritomo, Y.; Nakamura, A.; Kojima, N., Electronic Structure of the Gold Complexes $Cs_2Au_2X_6$ (X = I, Br, and Cl). *Phys. Rev. B* **1999**, *59*, 7925.

(14) Dong, L.; Sun, S.; Deng, Z.; Li, W.; Wei, F.; Qi, Y.; Li, Y.; Li, X.; Lu, P.; Ramamurty, U., Elastic Properties and Thermal Expansion of Lead-Free Halide Double Perovskite $Cs_2AgBiBr_6$. *Comput. Mater. Sci.* **2018**, *141*, 49-58.

(15) Xiao, Z.; Yan, Y.; Hosono, H.; Kamiya, T., Roles of Pseudo-Closed S2 Orbitals for Different Intrinsic Hole Generation between Tl-Bi and In-Bi Bromide Double Perovskites. *J. Phys. Chem. Lett.* **2017**, *9*, 258-262.

(16) Deng, Z.; Wei, F.; Brivio, F.; Wu, Y.; Sun, S.; Bristowe, P. D.; Cheetham, A. K., Synthesis and Characterization of the Rare-Earth Hybrid Double Perovskites:$(CH_3NH_3)_2KGdCl_6$ and $(CH_3NH_3)_2KYCl_6$. *J. Phys. Chem. Lett.* **2017**, *8*, 5015-5020.

(17) Ferreira, A.; Létoublon, A.; Paofai, S.; Raymond, S.; Ecolivet, C.; Rufflé, B.; Cordier, S.; Katan, C.; Saidaminov, M. I.; Zhumekenov, A., Elastic Softness of Hybrid Lead Halide Perovskites. *Phys. Rev. Lett.* **2018**, *121*, 085502.

(18) Songvilay, M.; Bari, M.; Ye, Z.-G.; Xu, G.; Gehring, P.; Ratcliff, W.; Schmalzl, K.; Bourdarot, F.; Roessli, B.; Stock, C., Lifetime-Shortened Acoustic Phonons and Static Order at the Brillouin Zone Boundary in the Organic-Inorganic Perovskite $CH_3NH_3PbCl_3$. *Phys. Rev. Mater.* **2018**, *2*, 123601.

(19) Kumar, N. R.; Radhakrishnan, R., Electronic, Optical and Mechanical Properties of Lead-Free Halide Double Perovskites Using First-Principles Density Functional Theory. *Mater. Lett.* **2018**, *227*, 289-291.

(20) Wei, F.; Deng, Z.; Sun, S.; Zhang, F.; Evans, D. M.; Kieslich, G.; Tominaka, S.; Carpenter, M. A.; Zhang, J.; Bristowe, P. D., Synthesis and Properties of a Lead-Free Hybrid Double Perovskite:$(CH_3NH_3)_2AgBiBr_6$. *Chem. Mater.* **2017**, *29*, 1089-1094.

(21) Deng, Z.; Wei, F.; Sun, S.; Kieslich, G.; Cheetham, A. K.; Bristowe, P. D., Exploring the Properties of Lead-Free Hybrid Double Perovskites Using a Combined Computational-Experimental Approach. *J. Mater. Chem. A* **2016**, *4*, 12025-12029.

(22) Sun, S.; Fang, Y.; Kieslich, G.; White, T. J.; Cheetham, A. K., Mechanical Properties of Organic–Inorganic Halide Perovskites, $CH_3NH_3PbX_3$ (X = I, Br and Cl), by Nanoindentation. *J. Mater. Chem. A* **2015**, *3*, 18450-18455.

(23) Sun, S.; Isikgor, F. H.; Deng, Z.; Wei, F.; Kieslich, G.; Bristowe, P. D.; Ouyang, J.; Cheetham, A. K., Factors Influencing the Mechanical Properties of Formamidinium Lead Halides and Related Hybrid Perovskites. *ChemSusChem* **2017**, *10*, 3740-3745.

(24) Debbichi, L.; Lee, S.; Cho, H.; Rappe, A. M.; Hong, K. H.; Jang, M. S.; Kim, H., Mixed Valence Perovskite $Cs_2Au_2I_6$: A Potential Material for Thin-Film Pb-Free Photovoltaic Cells with Ultrahigh Efficiency. *Adv. Mater.* **2018**, *30*, 1707001.